공학석사학위논문

Parametric Optimization for Power De-rate Reduction in Integrated Coal-fired Power Plant with CCS Retrofit

발전-포집-액화 통합 공정의 발전량 감소 개선을 위한 파라미터 최적화 연구

2015 년 2 월

서울대학교 대학원

화학생물공학부

안 진 주

Abstract

Parametric Optimization for Power De-rate Reduction in Integrated Coal-fired Power Plant with CCS Retrofit

Jinjoo An
School of Chemical & Biological Engineering
The Graduate School
Seoul National University

Carbon capture and storage (CCS) has attracted worldwide attention as a near-term technology to decelerate global warming. Especially, post-combustion CO_2 capture has an economic advantage by utilizing existing coal-fired power plants. Aqueous monoethanolamine (MEA) scrubbing is the most common post-combustion capture technology. However, the heat and energy requirements of solvent regeneration and CO_2 liquefaction cause the decrease in net power output up to 30 % by steam extraction and energy consumption. This power de-rate is a major obstacle to implementing CCS. In this study,

simulation-based parametric optimization of the operating conditions was performed to minimize the power de-rate. Post-combustion CO_2 capture with aqueous MEA scrubbing and CO_2 liquefaction integrated with a 550 MWe supercritical coal-fired power plant was simulated using Aspen Plus V7.3. The stripper operating pressure and liquid to gas ratio of CO_2 capture process were selected as the manipulated variables based on the variable evaluation. Steam extracted from IP-LP crossover pipe and the first LP turbine were considered as possible heat sources respectively. As a result, power de-rate was reduced from 38.3% to 17.4% when operating at optimum conditions.

Keywords: Power de-rate, CCS retrofit, Post-combustion CO_2 capture, Variable evaluation, Multivariable optimization, Parametric optimization

Student Number: 2013-20980

Contents

List of Figures

List of Tables

Nomenclature

$\Delta\alpha$	Difference between rich loading and lean loading
D	Power de-rate
η	Efficiency
J	Partial derivation of objective function
L	Lean solvent flow rate
$\dot{m}$	Steam flow rate
P_1	Pressure of inlet stream
P_2	Pressure of outlet stream
P_{str}	Operating pressure of stripper
R	Universal gas constant
γ	Ratio of heat capacities
T_1	Temperature of inlet stream
V	Molar volume
$\dot{W}$	Power generated by turbine work
x_i	Variable

Acronyms & Abbreviations

BT	Backup turbine
C	Compression
CCS	Carbon dioxide capture and storage
E	Energy
ECO	Economizer
FE	Flash evaporator
FWH	Feedwater heater

GHG	Greenhouse gas
HE	Heat exchanger
HEN	Heat exchanger network
HFE	Heated flash evaporator
HP	High pressure
IGCC	Integrated gasification combine cycle
IMTP	INTALOX® metal tower packing
IP	Intermediate pressure
L/G	Liquid to gas ratio
LP	Low pressure
MEA	Monoethanolamine
MTA	Minimum temperature approach
P	Pressure
RH	Reheater
Regen	Regeneration
SH	Superheater
T	Temperature
TTD	Terminal temperature difference
TVC	Thermal vapor compressor
USC	Ultrasupercritical

Subscripts

aux	Auxiliary
bt	Backup turbine
c	Condenser
comp	Compression

cond	Condensate
ex	Extracted steam
fg	Flue gas
fw	Feedwater
p	Pump
lean	Lean MEA solvent
R	Ratio
rich	Rich MEA solvent
str	Stripper
sat	Saturated

CHAPTER 1. Introduction

1.1. Research motivation

1.1.1. Current status of climate change

According to the report by the Intergovernmental Panel on Climate Change, global warming has been a major contributor to recent climate-related problems. Specifically, the energy supply sector is the largest greenhouse gas (GHG) source and accounted for approximately 35% of the total anthropogenic GHG emissions by 2010.[1] Among the many greenhouse gases, CO_2 is blamed for climate change because of its large total emission. Coal is considered one of the largest CO_2 emission sources in the energy sector and accounted for 40.58% of electricity generation in 2010, which is an amount that cannot be ignored. Furthermore, coal reserves are likely to last around 100 years at current rates of production. Owing to this abundance, it is highly possible that energy generation will continue to depend on coal-related power plants for a while. In the current situation of high dependency on coal, technology is needed that allows coal to be utilized for power generation while mitigating climate change. For this reason, carbon capture and storage (CCS) technologies have become an objective of research and attracted worldwide attention. By introducing CCS technology to the energy generation sector, existing conventional coal-fired power plants can maintain current coal usage while mitigating climate change.

In addition, extra time is provided for developing new and more eco-friendly technologies, such as integrated gasification combined cycle (IGCC) and ultra-supercritical (USC) power plants. Plants incorporating IGCC combust syn gas after removing CO_2 (pre-combustion CO_2 capture). Pre-combustion capture is known to be lower cost than post combustion CO_2 capture. USC power plants have lower coal consumption (320–340 g/kWh) and also lower values of CO_2 intensity factors (740–880 g CO CO_2/kWh) than conventional sub- and super-critical power plants.[2]

1.1.2. General description of the process

The CCS chain mainly consists of three processes: steam cycle, CO_2 capture, and liquefaction. During the steam cycle, pulverized coal is combusted in a boiler, and heat energy is absorbed by the boiler feedwater. Superheated steam is expanded through high, intermediate, and low pressure turbines connected to an electrical generator. At the same time, a small amount of steam is extracted from the inlet stream of each turbine in order to regenerate the feedwater. By doing so, the irreversibility of steam generation is reduced, and the thermodynamic efficiency of the steam cycle is improved.[3]

The types of CO_2 capture systems are post-combustion, oxy-fuel combustion, and pre-combustion. Capturing CO_2 from the flue gas produced by the combustion of fossil fuels in air is commonly involved in post-combustion capture.[4] In the post-combustion capture process, CO_2 is captured through a chemical reaction with a chemical solvent, such as monoethanolamine (MEA), in an absorber column and released in a stripper column by adding heat energy to break the CO_2-solvent bond. Between the two columns, hot CO_2-lean solvent leaving the stripper enters a heat exchanger to preheat cold CO_2-rich solvent, and is then fed back into the absorber column. CO_2 released from the solvent in the stripper is fed into the liquefaction process for shipping. There are many alternative processes for liquefaction using various refrigerants, such as ammonia and CO_2 itself. Among these processes, liquefaction by CO_2 itself is considered eco-friendly because no additional refrigerants are necessary. The

inlet stream is compressed to about 54 bar and then expanded. Gaseous CO_2 produced by this expansion has a temperature that is low enough to cool the CO_2 streams before they enter the compressors.

Unfortunately, the power de-rate is a significant issue when introducing the CCS process into an existing steam power plant. Figure 1 shows a conceptual diagram of a steam cycle with a CCS retrofit. The heat requirement for breaking the bond between the solvent and CO_2 is often met using steam extracted from a power plant. Steam extraction for solvent regeneration causes a decrease in net power output, and increases the amount of coal and power plants necessary to compensate this shortage. Consequentially, this process may actually increase CO_2 emission. Furthermore, the compression energy during the liquefaction process also increases the power de-rate. Therefore, reducing the power de-rate is key to CCS implementation and commercialization.

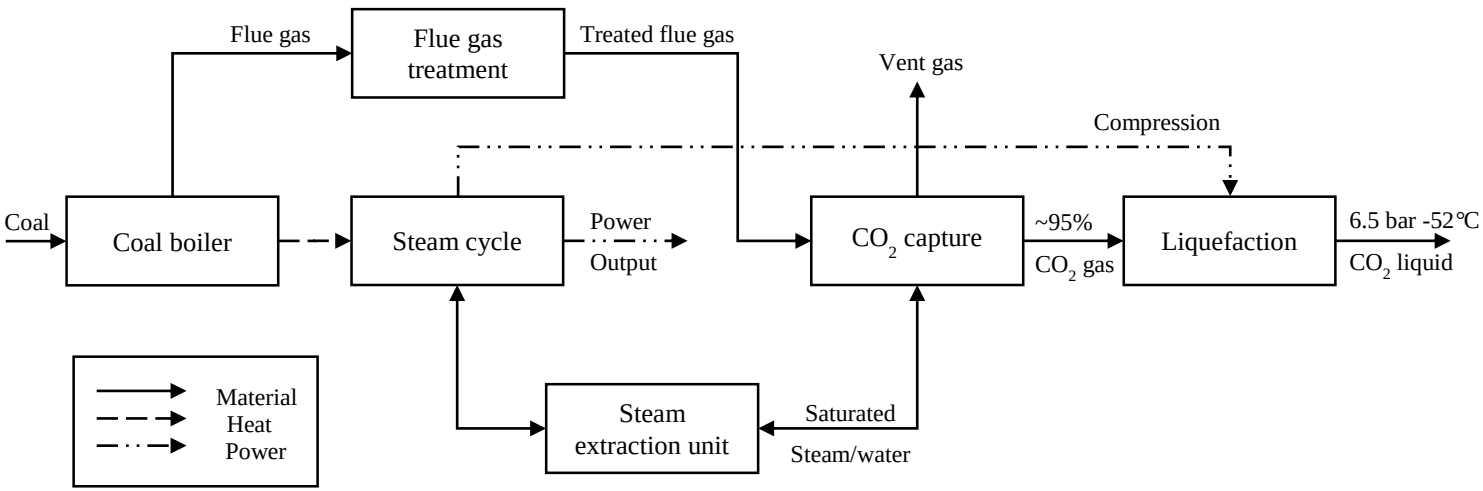

Figure 1. Conceptual diagram of integrated CCS process

1.1.3. Preceding research

As the steam extraction causes a sudden reduction in the steam flowrate in the turbines, the existing steam cycle is not operable. Moreover, the flue gas, which was originally sent to a stack, becomes the inlet gas of the CO_2 capture process. Some modifications of processes and equipment are therefore unavoidable. Some researchers have focused on retrofit options for using the steam cycle for steam extraction in order to minimize the power de-rate. Lucquiaud et al.[5] presented detailed options using the steam turbine and associated steam cycle designs and evaluated the plant efficiency for each option. Lucquiaud et al.[6] compared the retrofit costs of subcritical and supercritical power cycle plants and showed that the CO_2 abatement costs are the same for both. In addition, they showed that the plant efficiency has no intrinsic impact on the performance of the capture process if it is properly retrofitted and effectively integrated.

The reduction of the power de-rate by process and heat integration has been examined by some researchers. Harkin et al.[7] used pinch analysis and linear programming optimization to determine possible power de-rate targets in individual power plants and to reduce the overall power de-rate. Hanak et al.[8] investigated several heat exchanger network (HEN) designs for a high ash coal-fired power plant with CCS and proposed the use of flue gas for heating the boiler feedwater. Khalilpour et al.[9] reduced the power de-rate from 19.4% to 15.9% by heat integration of the flue gas with the reboiler and of the compressor

output with the feedwater regeneration. Liew et al.[10] analyzed capture module design options for heat and process integration, cooling, and the use of waste heat by HEN design and process modification.

Many researchers have also evaluated the power de-rate based on different operating scenarios. Sanpasertparnich et al.[11] studied the impact of coal rank, steam extraction location, and flue gas load on CO_2 capture efficiency. Dave et al.[12] performed case studies on the plant efficiencies of existing coal-fired power plants (subcritical and supercritical) and new coal-fired power plants (subcritical, supercritical, and ultra-supercritical) by evaluating the CO_2 capture demand and cooling options. Liang et al.[13] conducted an optimization of some important process parameters, including the operating stripper pressure, CO_2 capture efficiency, and steam extraction location. Cifre et al.[14] reported the influence of important parameters on the power de-rate and analyzed the power de-rate with different solvents. Eslick et al.[15] performed a multi-objective evaluation of a coal-fired power plant with CCS to minimize water consumption and the levelized cost of electricity by using the surrogate model to simplify the optimization problem.

In addition, modified configurations and methods for power de-rate prediction and reduction have been proposed. Van Peteghem et al.[16] developed an analytical framework that can provide insight on the influence of solvent storage systems and the electricity market by using electricity price (peak and off-peak) to regenerate stored solvent. Patiño-Echeverri et al.[17] analyzed the

profitability of amine storage systems using historical regional electricity price differentials in the US. Liebenthal et al.[18] proposed correlations to predict the impact of heat duty on solvent regeneration and cooling, and the electricity duty on CO_2 capture and compression. Zhang et al.[19] proposed two improved capture systems: the flash evaporator (FE) with thermal vapor compressor (TVC) and the heated flash evaporator (HFE) with TVC. These systems used high-temperature condensate from the stripper reboiler in the capture process and reduced the power de-rate up to 1%. House et al.[20] suggested a temperature swing separation system to reduce the amount of additional fuel that is necessary to compensate for the energy shortage caused by the power de-rate. Liang et al.[13] proposed a bi-pressure stripper to minimize the power de-rate for CO_2 capture and compression.

1.2. Research objectives

The main objective of the thesis is to minimize the power de-rate of a retrofitted coal-fired power plant integrated with CO_2 capture and liquefaction processes by parametric optimization of process operating conditions. Even though the energy requirement for each unit process is at minimum level, nonlinearity between variables makes the integrated system difficult to predict the power de-rate according to change in operating conditions. Therefore, the thesis aims at following objectives:

- to develop each unit process based on the literature and the data for 0.1 MW capture pilot plant modeling
- to evaluate the influence of possible manipulated variables on the power de-rate
- to show the influence of the extracted steam condition and of steam extraction unit alternatives on the power de-rate
- to minimize the power de-rate by manipulating selected variables
- to discuss nonlinearity of influential variables to achieve much insight in the overall process

1.3. Outline of the thesis

The thesis is divided into five chapters. Chapter 1 describes the motivation and the objectives of the thesis. The current status of climate change and preceding research are introduced. Chapter 2 describes the development of simulation models of a steam cycle, CO_2 capture, and liquefaction processes in detail. Chapter 3 describes the integration of aforementioned process models of a coal-fired power plant with aqueous monoethanolamine (MEA) scrubbing and liquefaction. The manipulated variables are selected by variable evaluation to the power de-rate. Chapter 4 discusses the results of parametric optimization to minimize the power de-rate and relationships between the variables with the power de-rate. Lastly, chapter 5 presents the conclusion of the thesis.

CHAPTER 2. Process description

The steam cycle, CO_2 capture process, and liquefaction process were used in this study. To make a comparison to a case with optimum conditions, a base case process was first investigated. In this section, a general description of the processes that were employed is presented. The simulation was performed with ASPEN Plus V7.3.

2.1. Description of steam cycle

A 550 MWe air-based supercritical steam cycle was used for this study. The process specifications were based on a DOE/NETL report.[21] The steam cycle flow diagram is shown in Figure 2. The property method was STEAMNBS, which that uses the NBS/NRC steam tables to calculate any thermodynamic properties of water.[22] The model consists of two high pressure (HP), two intermediate pressure (IP), and five low pressure (LP) turbines, as well as seven feedwater heaters (FWHs), condensers, and condensate pumps. Feedwater is first evaporated into high pressure and temperature steam by passing through an economizer (ECO-L) and superheater (SH-L). The generated steam flows through two stages of HP turbines. Following the HP turbines, the steam enters a re-heater (RH-L) to recover more heat energy from a boiler, and then flows to the IP and LP turbines in sequence and is finally condensed (CONDENSER). Part of the turbine energy is converted into mechanical energy by rotating

electrical generator. Condensed feedwater is pumped back to the economizer by a condensate pump. During delivery, the feedwater is passed along feedwater heaters, which are heat exchangers that increase the temperature of the feedwater using the latent and sensible heat of a small amount of extracted steam. Steam is extracted from every stage of the turbines (multistage extraction). The amount of steam to be extracted is decided based on the terminal temperature difference (TTD), defined as equation (1).

$$TTD = T_{sat} - T_{fw} \quad (1)$$

T_{sat} is the condensing temperature of the steam extracted and T_{fw} is the temperature of the feedwater leaving the feedwater heater. By regenerating the feedwater, the irreversibility of the system involving steam generation is reduced, thus the thermodynamic efficiency is improved. In this model, a closed feedwater heater is assumed.[3] The TTD values are determined for each turbine using the values of the model in the DOE/NETL report.[21] The LP steam from the last stage turbine is in vacuum condition (0.069 bar and 38.7 ℃). The flue gas generated from the pulverized coal boiler is sent directly to the CO_2 capture process. Any pressure drops in heat exchangers and pipelines are ignored. The detailed design specifications and simulation results are listed in Table 1.

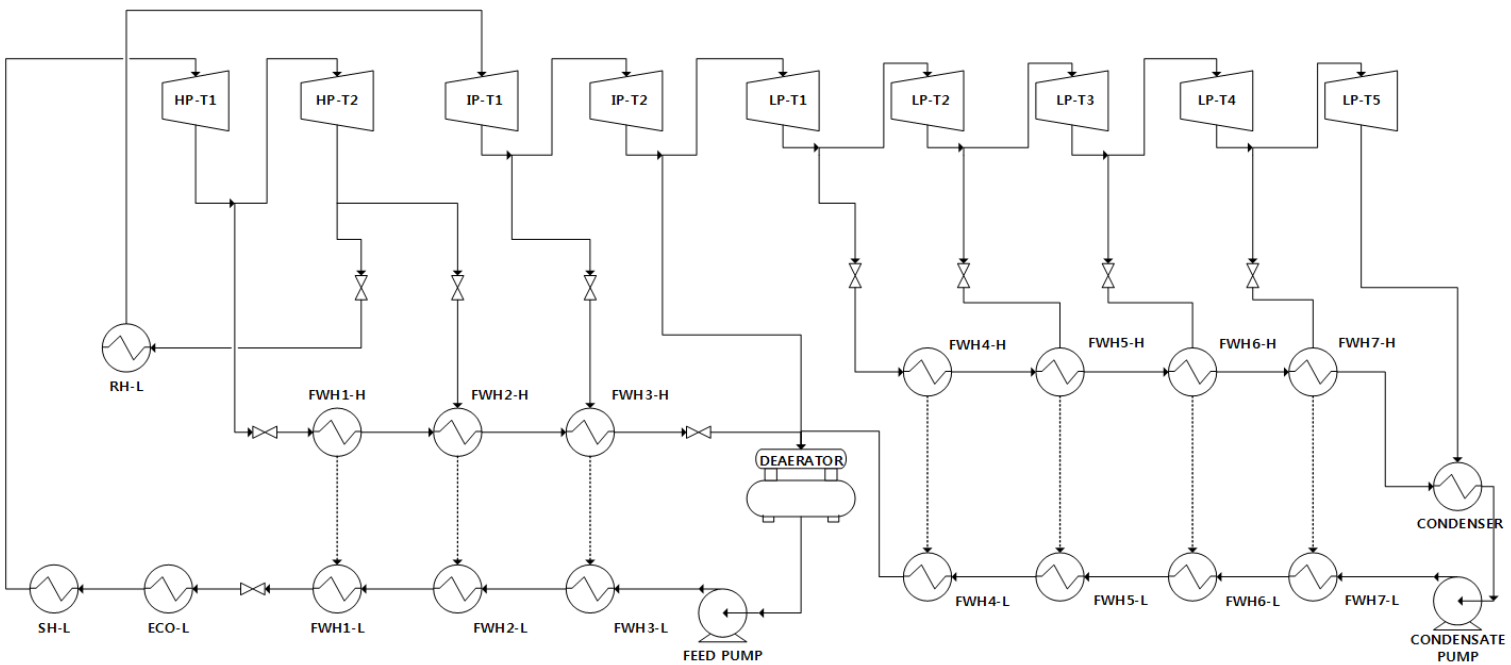

Figure 2. Process flow diagram of a 550 MWe steam cycle

Table 1. Design specifications and simulation results for the steam cycle

Net plant power	550 MWe
Net plant efficiency (LHV)	39.4%
Turbine discharge pressure, bar	
High Pressure	76.91 / 49.01
Intermediate Pressure	21.38 / 9.49
Low Pressure	5.012 / 1.324 / 0.579 / 0.241 / 0.069
SH steam	242.35 bar, 598.89 ℃
RH steam	49.01 bar, 621.1 ℃
TTD, ℃	
FWH1	-1.084
FWH2	-0.023
FWH3	-1.113
FWH4	2.803
FWH5	2.747
FWH6	2.7637
FWH7	2.7542
Turbine power output, MWe	
High Pressure	146.3 / 39.7
Intermediate Pressure	93.1 / 72.6
Low Pressure	42.9 / 69.0 / 35.2 / 31.1 / 36.7
Auxiliary load [1], MWe	16.7

[1] $W_{aux} = W_{p,cond} + W_{p,fw}$

2.2. Description of CO_2 capture process

2.2.1. Description of the conventional MEA scrubbing for CO_2 capture

A typical CO_2 capture process with an absorber and a stripper with a lean-rich solvent heat exchanger was used for this study, as indicated in Figure 3. As flue gas from coal-fired power plants has a low concentration and partial pressure of CO_2, chemical absorption is more suitable than physical absorption.[23] Aqueous MEA was selected for the chemical solvent. Acid gas removal using MEA has been studied over the last decades; thus, much of the MEA data needed for the simulation are easily obtained from the literature. Furthermore, one main focus of this study is to optimize the process operating condition without modifying the process itself, and MEA fits well with this goal.

The flue gas generated from the boiler is cooled to 40 ℃ before entering the bottom of the absorber. In the absorber, cold lean MEA is fed to the top of the column and selectively absorbs CO_2 by an exothermic chemical reaction. Cold CO_2-rich MEA solvent is drained out from the bottom of the column. The remaining flue gas is sent back to the stack and purged to the atmosphere. Cold rich MEA solvent is preheated in the lean-rich MEA heat exchanger and is fed to the top of the stripper column. The hot rich MEA solvent desorbs CO_2 by an endothermic reaction at high temperature and is then drained out from the bottom of the stripper. The vapor is cooled by the stripper condenser and gaseous captured CO_2 is ready for the liquefaction process. The hot lean MEA

drained from the stripper is sent to the lean-rich MEA heat exchanger to be cooled and then sent back to the absorber column as the cold lean MEA solvent.

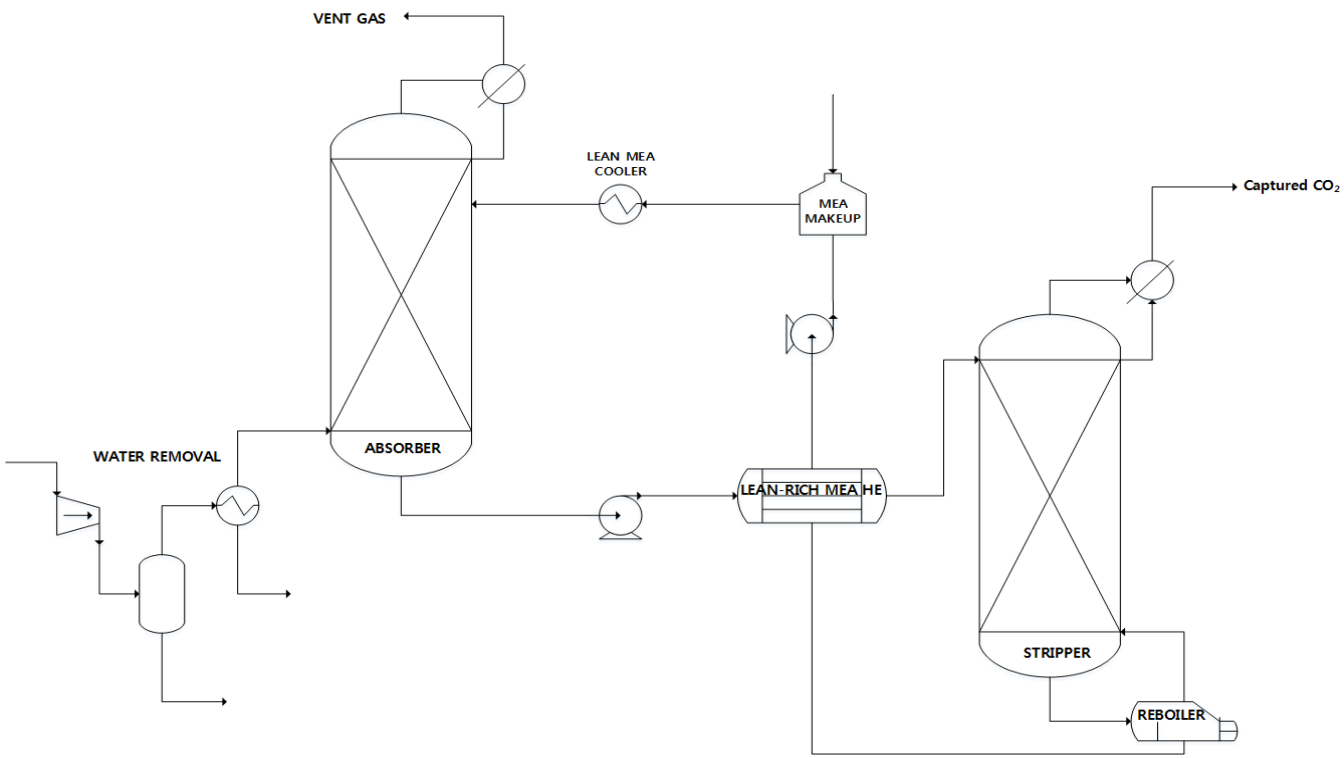

Figure 3. Conventional post-combustion CO_2 capture process flow diagram

2.2.2. Simulation specifications of CO_2 capture model

The specifications of the simulation were based on the data from a 0.1 MW CO_2 capture pilot plant in Boryeong, Republic of Korea, which was built by the Korea Electric Power Corporation (KEPCO) and the Korea Midland Power Corporation (Figure 4). Detailed information on the plant specifications are listed in Table 2 and the major process operation indicators are presented in Table 3. The capture efficiency of the plant is 90% CO_2 removal when 30 wt% aqueous MEA is used as the amine solvent, and the heights of the absorber and the stripper are 16.8 m and 11.25 m.

Based on the data from the pilot plant, a 550 MW CO_2 capture model was developed assuming 90% CO_2 removal with 30 wt% MEA the solvent. A rate-based Radfrac model with film theory was used for the absorber and the stripper, and Intalox Metal Tower Packing (IMTP) was selected as a packing material. To appropriately establish the model, mass transfer coefficient and interfacial area methods were used. The interfacial area factors for the absorber and the stripper were 0.7 and 0.5, respectively, and the Henley IMTP model was used to predict the column temperature profile. The Electrolyte-NRTL model was employed to estimate the thermodynamic properties of the MEA–H_2O–CO_2 system. To calculate the reaction kinetics of MEA–H_2O–CO_2, a kinetic model suggested by Hikita et al.[24] was used. A summary of the process specifications are shown in Table 4. MEA degradation at temperatures lower than 120 ℃ was

assumed to be negligible. This process was assumed to handle 100% of the flue gas from the 550 MWe power plant; detailed information for the flue gas[21] is listed in Table 5.

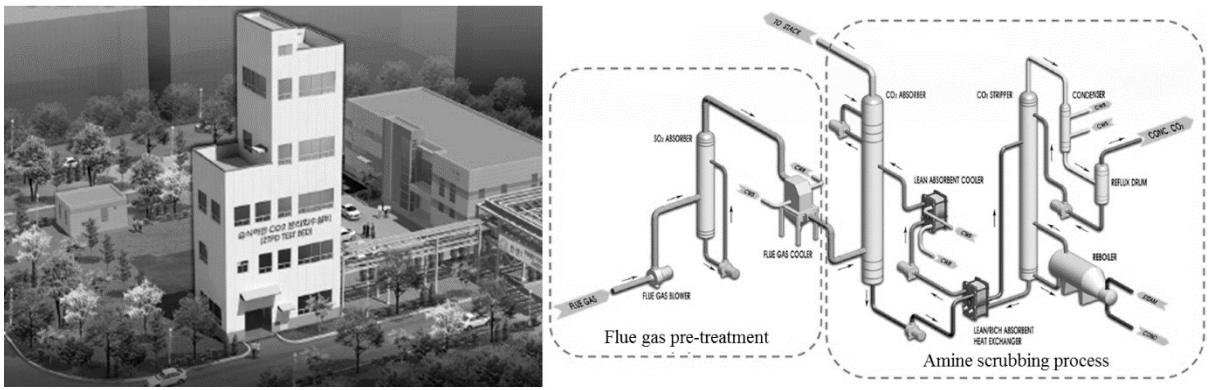

Figure 4. A 0.1 MW CO_2 capture pilot plant in Boryeong, Republic of Korea

Table 2. Specifications of a 0.1 MW CO_2 capture pilot plant

Feed conditions	
Temperature	43.0 ℃
Pressure	0 barg
Flowrate	331.8 Sm^3/hr
Composition	dry-vol %
N_2	80.81
CO_2	14.90
O_2	4.29
SO_2	4.4 ppmdv
Lean amine temperature	40.0 ℃
Lean amine flowrate	1,235 L/hr
Lean amine concentration	30.0 wt.%
Absorber	
Temperature (top)	40.0 ℃
Pressure (top)	0.018 barg
The height of column	16.8 m
Stripper	
Temperature (top)	83.4 ℃
Pressure (top)	0.5 barg
The height of column	11.25 m

Table 3. Operation results for a 0.1 MW CO_2 capture pilot plant

Process Indicators	
Capture efficiency	89.74 %
Capture capacity	1.91 ton/day
L/G ratio	3.7 L/Sm^3
Regeneration energy	3.99 GJ/tonCO_2
Cooling water	63 m3/tonCO_2
MEA solvent circulation flowrate	15.5 m3/tonCO_2
Utility	
Steam flowrate	150 kg/hr
Cooling water	9.7 m^3/hr
Auxiliary power consumption	40.0 kW

Table 4. Design specifications of a 550 MW CO_2 capture process (base case)

Capture efficiency	90 %
MEA Solvent	
Concentration	30 wt.%
Lean solvent loading	0.228 mol CO_2/mol MEA
Rich solvent loading	0.567 mol CO_2/mol MEA
Absorber	
Temperature (top)	40.0 ℃
Pressure (top)	1.01 bar
The height of column	37 m
Stripper	
Temperature (top)	82.0 ℃
Pressure (top)	1.01 bar
The height of column	8 m
Lean-rich solvent heat exchanger	
Minimum temperature approach (MTA)	9 ℃

Table 5. Properties of the flue gas flowing into the capture process [21]

Molar flowrate	162,877 lbmol/hr
Temperature	57 ℃
Pressure	0.1 MPa
Composition	mole fraction
H_2O	0.1517
CO_2	0.1353
N_2	0.6808
O_2	0.024
Ar	0.0082

2.3. Description of CO_2 liquefaction model

The simulation model for the liquefaction process was built based on the report of Lee et al.[25] The liquefaction model proposed by Lee et al. consumed a minimum compression energy of 98.1 kWh/t CO_2.

Figure **5** shows the process flow diagram for the liquefaction model. Soave-Redlich-Kwong (SRK) was used as the property method with a modified binary interaction parameter (k_{ij}) of 0.193 in the van der Waals mixing rule.[26] Captured CO_2 is fed to a seawater heat exchanger (SEAWATER HE-1) to reduce the temperature before entering the multistream process heat exchanger (PROCESS HE-1). Cold gaseous CO_2 cools down the inlet CO_2 to remove H_2O contained in the inlet stream through condensation. Compressors and seawater heat exchangers are used to cool and compress CO_2 up to 54.4 bar. Between each stage, the stream is reduced in temperature by being fed to a process heat exchanger (PROCESS HE-2). Before entering the compressors, flash separators (FLs) drain out any liquid phase to protect the compressors. The drained liquid (mainly water) is fed back to the first flash separator (FL-1) and water is removed from the system. The compressed CO_2 stream is fed to a seawater condenser (CONDENSER), and then goes through multistage expansion. The cold CO_2 gas generated by expansion is used to decrease the temperature of the streams in the multistream process heat exchangers (PROCESS HE), and then fed back to the compressors. Finally, cold liquefied CO_2 is obtained at the target conditions (6.5 bar and -52 ℃). The major process

parameters and input stream composition are listed in Table 6. More detailed descriptions of the process are available in the literature.

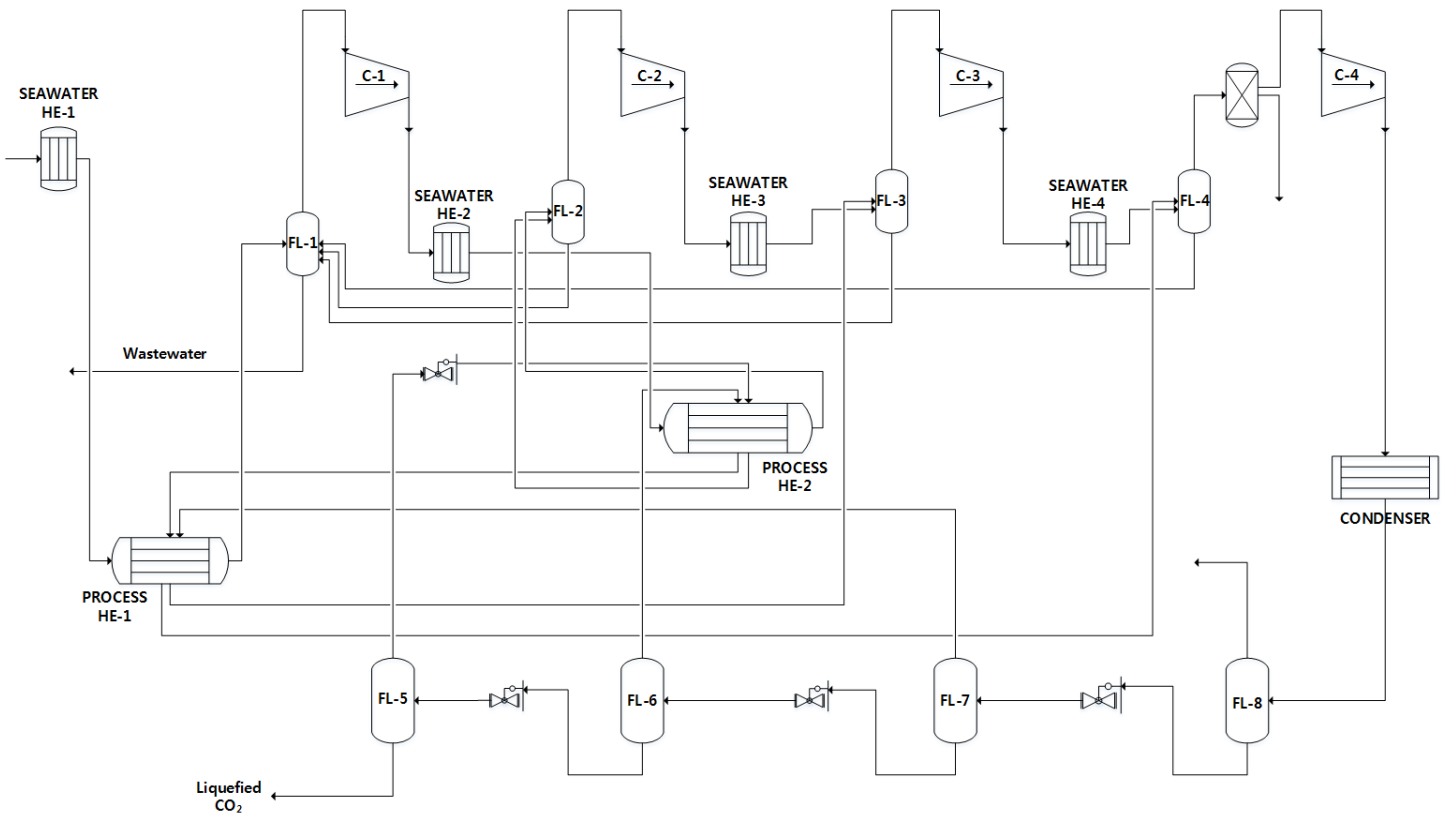

Figure 5. CO_2 liquefaction process flow diagram

Table 6. Design specifications of the CO_2 liquefaction process

Target CO_2 product	
Temperature	-52 ℃
Pressure	6.5 bar
Compressor efficiency	82 %
Pump efficiency	85 %
Process heat exchanger	
Minimum temperature approach	3 ℃
Seawater heat exchanger	
Minimum temperature approach	5 ℃
Seawater temperature	10 ℃
Input stream composition (base case)	
CO_2	92.46 mol%
H_2O	7.48 mol%
Volatiles	0.06 mol%
Compressor outlet pressures (base case)	2.78 / 7.73 / 21.49 / 54.4

CHAPTER 3. Integration of steam cycle with CO_2 capture and liquefaction processes

3.1. Definition of power de-rate

To introduce CCS processes into existing steam cycles, a heat source should be supplied to a reboiler of the stripper for solvent regeneration. Unfortunately, the reboiler of the stripper is known to be an energy intensive unit and one of the main obstacles to CCS implementation. Among the many methods for supplying heat to a reboiler, it is advantageous to use steam extracted from the steam cycle. This is not only because building a CO_2 capture plant near the power plant reduces the cost of flue gas transport, but also because the steam cycle is relatively abundant in low pressure and temperature steam. However, the steam has to be depressurized and reduced in temperature because the stripper reboiler uses only the latent heat in exchanging heat. The compression energy in the liquefaction process also decreases the net plant power. The inevitable plant efficiency penalty from extracting steam for the stripper reboiler and compression energy is reported to reach 30%.[27,28] This is the so-called "power de-rate" (*D*) and is calculated using the following equation (2).

$$\boldsymbol{Power\ derate(D) = 1 - \frac{Net\ plant\ power\ with\ CCS}{Net\ plant\ power\ without\ CCS}} \qquad (2)$$

An increase in the power de-rate means a power plant produces less energy than the original power plant with the same amount of coal. Thus, the power de-rate can be used as an indicator of operational economics.

3.2. Steam extraction from an existing power plant

Figure **6** shows possible locations for steam extraction and the pressures at these locations. Among these locations, there are two suitable locations in the steam turbines to extract steam: the IP-LP crossover pipe (D) and the first low pressure turbine (E). The higher temperatures and pressures before the crossover pipe are too high, whereas after the first LP turbine the temperatures and pressures too low to use as hot stream in a stripper reboiler. Finding an optimum steam extraction point is important to avoid extracting steam with unnecessarily high temperature and pressure and minimize the power de-rate.

A steam extraction unit is necessary to obtain suitable conditions for the reboiler. Figure **7** shows alternatives to the steam extraction unit. Steam extraction units consist of three pieces of equipment: depressurizer ((a) valve and (b) turbine), desuperheater, and saturated water pump. The depressurizer and desuperheater vary the pressure and temperature of the extracted steam to be suitable for a reboiler. Basically, only the latent heat of the steam can be used for solvent regeneration in the reboiler. For example, if the temperature at the reboiler is 102.4 ℃, the pressure of steam should be 1.56 bar as saturated steam when considering the 10 ℃ minimum temperature approach (MTA) of a reboiler. However, since the steam pressures from the IP-LP crossover pipe and first LP turbine are 9.5 and 5.0 bar, respectively, the steam should be reduced in pressure and temperature. Following depressurization to the required pressure, steam is still in superheated. The desuperheater reduces the

temperature of the steam to the saturation temperature. Furthermore, MEA thermal degradation and the power de-rate can be decreased by using the minimum temperature of steam for reboiler. As steam pressure increases, the amount of latent heat per unit mass decreases, which means more steam has to be extracted because the steam is a wet fluid. Because the work done by the steam turbines is theoretically proportional to the steam flow rate, as indicated equation (3), decreasing steam extraction directly reduces the power de-rate. Lastly, a saturated water pump is used after the steam is saturated in the reboiler to pump the condensate back into the steam cycle.

$$\dot{W} = \dot{m}\eta \frac{\gamma R T_1}{\gamma - 1}\left[\left(\frac{P_2}{P_1}\right)^{(\gamma-1)/\gamma} - 1\right] \quad (3)$$

It is obvious that depressurizing using a backup turbine (b) can recover some energy from the extracted steam and reduce the power de-rate. However, a backup turbine (b) costs much more than a reducing valve (a) in both purchase and installation costs for the turbine itself and the electric generator. Therefore, it is necessary to consider both cases ((a) and (b)) for the purpose of future work and economic analysis.

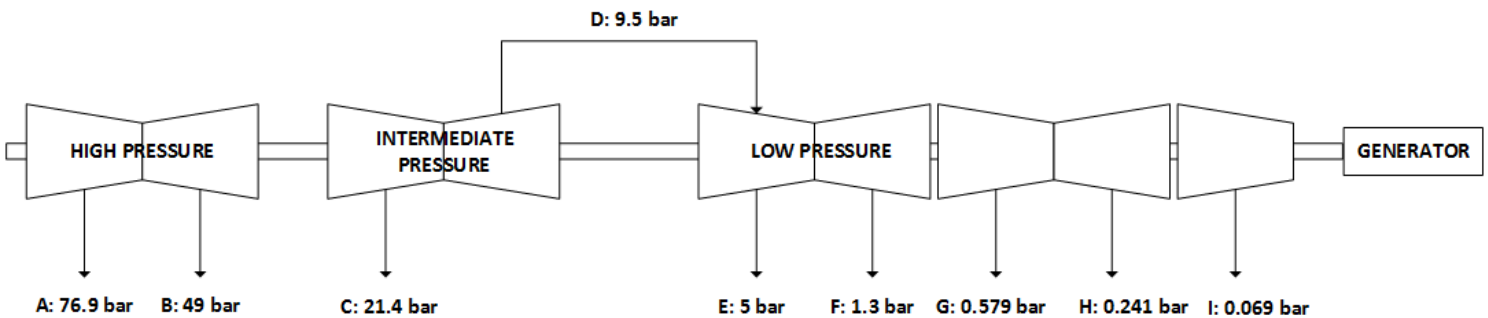

Figure 6. Possible steam extraction locations: (A, B) high pressure steam, (C) intermediate pressure steam, (D) IP-LP crossover steam, (E–I) low pressure steam

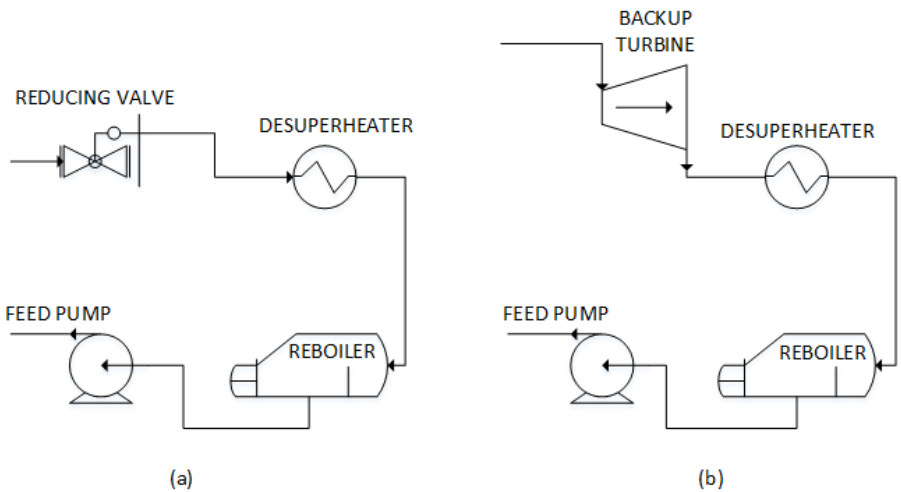

Figure 7. Alternatives for steam extraction unit: (a) Reducing valve, (b) Backup turbine

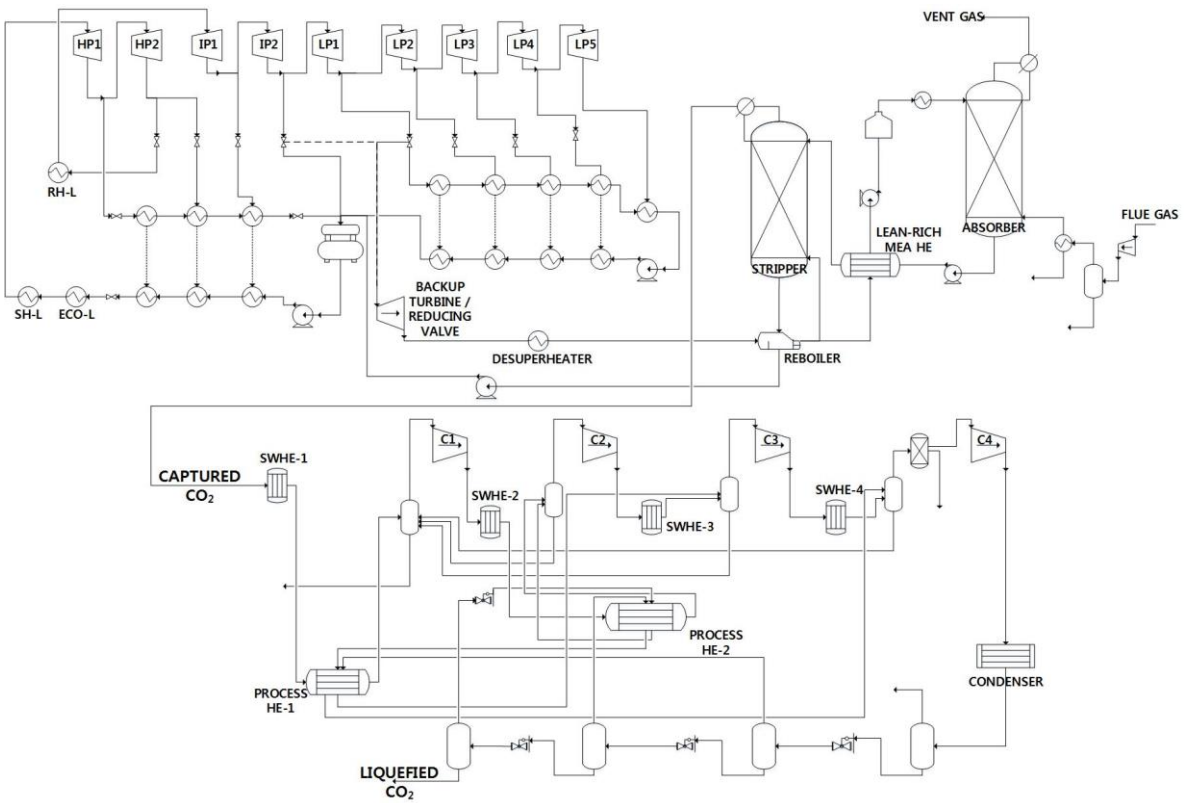

Figure 8. Flow diagram of the integrated CCS process

3.3. Variable selection

The power de-rate (D) of a power plant can be expressed using several parameters and variables of the three processes as equation (4).

$$\boldsymbol{D = f(x_i)} \tag{4}$$

The following variables (x_i) possibly influence the power de-rate.

- CO_2 capture process: temperature of flue gas (T_{fg}), liquid to gas ratio (L/G), stripper operating pressure (P_{str}), temperature of lean solvent (T_{lean}), temperatures of condensers of absorber and stripper (T_c), minimum temperature approach (MTA) of lean-rich heat exchanger
- CO_2 liquefaction process: pressure ratio of compressors (C_R)

The MTA of the lean-rich heat exchanger was excluded because there is no constraint on temperature in the hot-rich solvent stream in the model used. If minor solvent evaporation in the rich solvent stream by heat exchange is ignored, it is obvious that a small MTA value is beneficial for the absorption of more heat from the hot-lean solvent. Parameter evaluation was performed to investigate the influence of each parameter and to decide which parameters should be included in the analysis. The above parameters were assigned $x_1 = T_{fg}$, x_2 = L/G, $x_3 = P_{str}$, $x_4 = T_{lean}$, $x_5 = T_{c,abs}$, $x_6 = T_{c,str}$, and $x_7 = C_R$ and the degree of influence on the power de-rate is expressed as the following equation (5).

$$\boldsymbol{J = \frac{\partial D}{\partial x_i}} \tag{5}$$

By evaluating the degree of a change in the power de-rate by manipulating a selected variable, it is possible to determine if the variable has a dominant influence on the objective. If $\partial D / \partial \mathrm{x}$ is close to zero, it has little impact on the power de-rate within a chosen range. Evaluation was performed at the operating conditions of the 0.1 MW capture pilot plant. The results of the variable evaluation showed that x_1, x_4, x_5, and x_6 had no net effect on the power de-rate, whereas x_2, x_3, *and* x_7 were relatively influential. However, because the effect of x_7, compression ratios, on the power de-rate was negligible compared with that of x_2 and x_3, it was not considered further. As a result, P_{str} and L/G were selected as the manipulated variables. The results of the variable evaluation are listed in the Table **7**.

Table 7. Results of variable evaluation

Variables	Evaluation at	$J\ (\times 10^{-1})$	Unit
CO_2 capture			
Stripper pressure	1.5 bar	5.87	%/bar
L/G	3.5 L/m^3	1.12	%/(L/m^3)
Flue gas cooling temp.	40 ℃	0.12	%/℃
Lean amine cooling temp.	40 ℃	0.00	%/℃
Absorber condenser temp.	40 ℃	0.02	%/℃
Stripper condenser temp.	40 ℃	0.00	%/℃
Liquefaction			
Compression ratio [1]		0.64	%

[1] J for compression ratio is calculated by optimization problem

CHAPTER 4. Results and discussion

4.1. CO_2 capture process

4.1.1. Effects of stripper operating pressure

The operating pressure of the stripper not only affects the solvent regeneration energy but also determines the inlet pressure of the liquefaction process, that is, the compression ratios of four compressors and the compression energy. Consequently, the power de-rate is mainly influenced by the operating pressure of the stripper, which is the sole parameter that directly concerns the overall integrated process. A simulation for calculating the power de-rate was performed by manipulating the stripper operating pressure without changing the L/G value. The operating range was set from 1 to 2 bar based on the reboiler temperature. Rochelle[29] reported that MEA loss owing to thermal degradation mainly occurs in the reboiler and reboiler sump, and that the higher temperature of the stripper lowers not only the energy requirement of the stripper but the capital cost of the stripper column and compressors. Therefore, the operating condition range of the stripper is solely determined by thermal degradation of the solvent. Although Davis[30] proposed an operating pressure of 3 bar and 132 ℃ for 30 wt% MEA, many CO_2 capture systems with aqueous MEA have been designed to operate at a maximum temperature of 120 ℃, which is equivalent to ~2 bar in the system used in this study.

Figure 9 clearly shows the overall effect of changing the operating pressure of the stripper. In the CO_2 capture process, an increased operating pressure tends to decrease the solvent regeneration energy and elevate the temperature at the reboiler of the stripper. The result of the base case CO_2 capture process is 5.03 GJ/tonCO_2 regeneration energy and a reboiler temperature of 102.7 ℃. The regeneration energy (Figure **9** (b)) is sharply decreased to 3.84 GJ/tonCO_2 for an operating pressure of 1.25 bar and then stabilizes at about 3.3 GJ/tonCO_2 as the operating pressure of the stripper is further increased.

Based on the result of the simulation for the CO_2 capture and liquefaction processes, the power de-rate was calculated for steam extraction at the IP-LP crossover pipe and the first LP turbine, as shown in Figure 10. The power de-rate was higher using pressure reducing values compared with using backup turbines. Moreover, steam extraction at the IP-LP crossover pipe resulted in a higher power de-rate than using steam from the first LP turbine with pressure reducing valves. In base case, the power de-rates for extraction at the IP-LP crossover pipe and LP turbine were 38.3% and 32.4%, respectively. However, with backup turbines the IP-LP crossover pipe steam had a slightly lower power de-rate than the LP steam (21.4% and 21.9%, respectively). Therefore, the steam extraction location can be determined by other factors, such as capital cost, easiness of retrofit, or modifiability of the process control to use an additional backup turbine. Detailed results are listed in Table **8**.

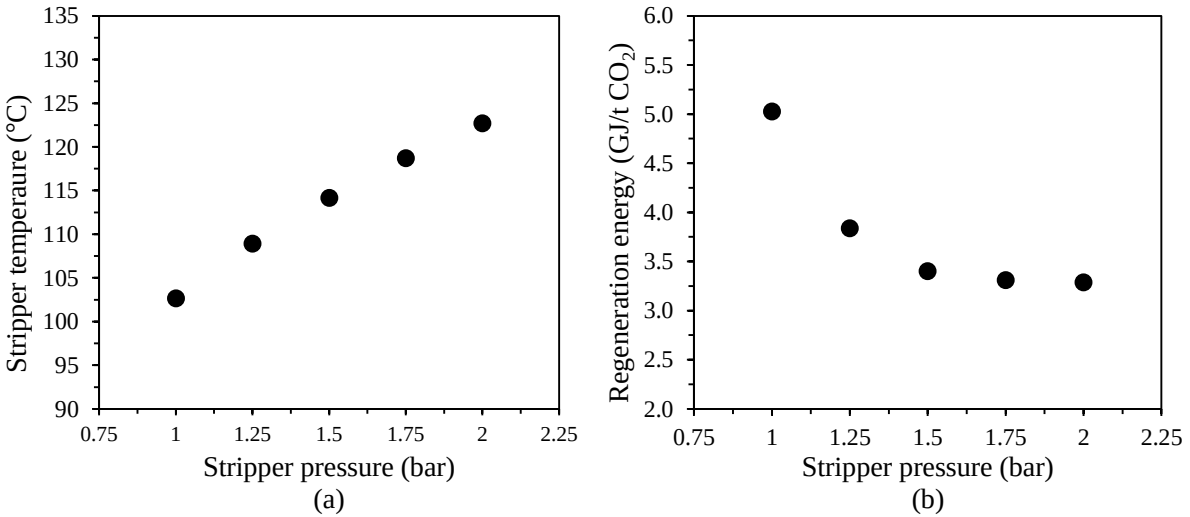

Figure 9. Simulation results for the effect of the stripper operating pressure on (a) the stripper temperature and (b) the regeneration energy

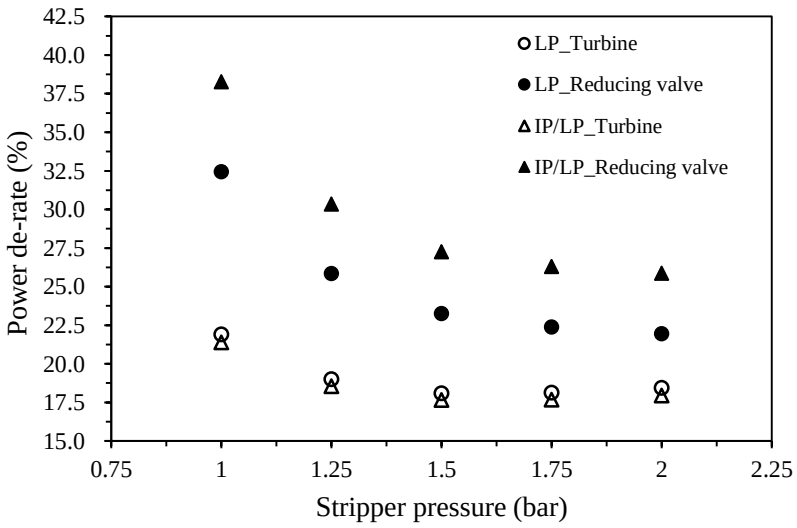

Figure 10. Simulation results for the effect of the stripper operating pressure on the power de-rate of the steam cycle

Table 8. Simulation results varying stripper pressure

Stripper pressure	1	1.25	1.5	1.75	2
CO_2 capture					
RB Temperature, ℃	102.7	108.9	114.2	118.7	122.7
Regen. E, GJ/tonCO_2	5.03	3.84	3.40	3.31	3.29
Solvent, m^3/tonCO_2	13.58	13.58	13.59	13.59	13.59
Liquefaction					
Power consumption, MW	38.5	36.1	34.3	32.5	31.1
Steam cycle					
Steam pressure, bar	1.57	1.92	2.3	2.60	2.93
Steam flowrate, ton/hr	896	689	615	602	601
Net Power out, MW					
IP-LP crossover pipe					
Reducing valve	378.0	419.2	434.4	437.8	438.8
Backup turbine	470.9	484.0	487.2	485.3	482.4
First LP turbine					
Reducing valve	410.1	443.9	456.4	459.4	460.3
Backup turbine	468.0	481.5	484.8	482.7	479.6
Power de-rate *J*, %					
IP-LP crossover pipe					
Reducing valve	38.3	30.3	27.3	26.3	25.9
Backup turbine	21.4	18.6	17.7	17.7	17.9
First LP turbine					
Reducing valve	32.4	25.9	23.3	22.4	22.0
Backup turbine	21.9	19.0	18.1	18.2	18.5

4.1.2. Effect of liquid to gas ratio (L/G)

The liquid to gas ratio in the capture process is the amount of lean amine solvent supplied compared with the amount of incoming flue gas to the absorber; this variable is solely influential in the capture process. As the amount of incoming flue gas was constant in the used model, L/G can be explained solely with the lean amine solvent flow rate (liquid, L) and the amount CO_2 held in the lean amine solvent (lean loading). Explanations of L/G often involve $\Delta\alpha$, which is the difference between rich loading and lean loading; however, rich loading is dependent on the amine flowrate and lean loading to satisfy a targeted amount of CO_2, as shown in the following simplified equations (6) and (7).

$$\dot{m}_{CO_2} = \dot{m}_{MEA}\Delta\alpha \tag{6}$$

$$\Delta\alpha = \alpha_{rich} - \alpha_{lean} \tag{7}$$

Figure 11 shows the simulation result for the regeneration energy when L/G is manipulated at fixed stripper operating pressures from 1 to 2 bar. The regeneration energy is first reduced by increasing L/G until an optimum value is reached when the slope of the curve is near zero, and then the regeneration energy slightly increases at higher L/G values. The regeneration energy is more affected by L/G at the lower stripper pressure. At 1 bar, the regeneration energy varies from 11.6 to 3.77 GJ/tonCO_2, whereas it varies from 3.93 to 3.27 GJ/tonCO_2 at 2 bar. This result means that it is critical to operate the capture

process near the optimum L/G for a stripper operating pressure to minimize the regeneration energy and power de-rate, especially at lower stripper pressures.

As the stripper operating pressure increased, the optimum L/G was observed at lower values. For example, at 1 bar, the minimum regeneration energy was observed at L/G of 4.51 L/m^3, whereas at 2 bar, the minimum value was observed at L/G of 3.24 L/m^3. The lowest regeneration energy was 3.27 $GJ/tonCO_2$ at L/G of 3.24 L/m^3 and a stripper operating pressure of 2 bar.

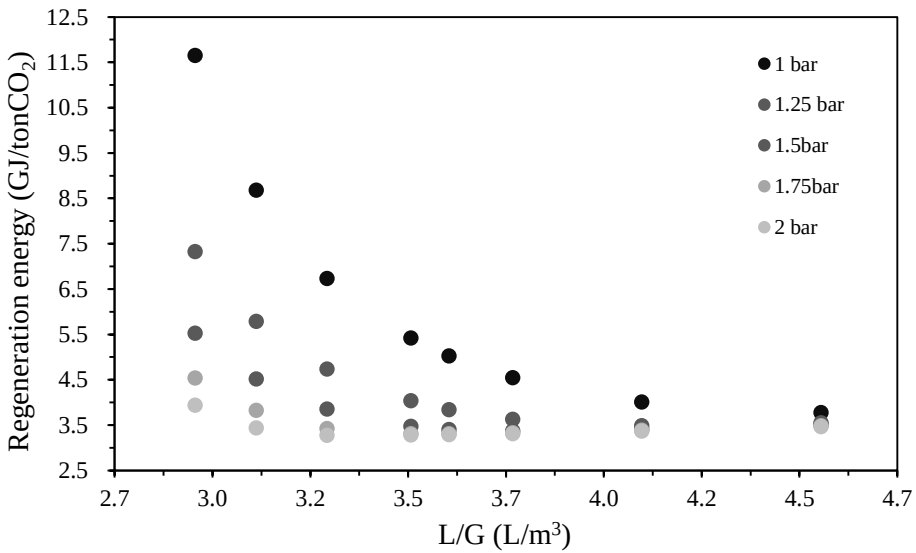

Figure 11. Simulation results for the effect of liquid to gas ratio on the regeneration energy

4.2. Liquefaction process for shipping

A major energy consumer in the liquefaction process is the compression. The compression energy is mainly determined by the compression ratio (P_2/P_1) and flowrate ($\dot{m}$), as indicated in equation (3). The inflow rate to the first compressor is determined by the pressure and temperature of the inflow gas. The amount of CO_2, which is the majority of the inflow species, is a constant value set by the design specifications of the CO_2 capture process and is independent of the stripper pressure. However, the composition of the inflow is determined by the mixture vapor-liquid-equilibrium (VLE) at a certain pressure and temperature (partial condenser, 40 ℃), and the total inflow rate varies, mainly owing to the amount of H_2O. Furthermore, the composition of the inflow gas is not significantly changed by manipulating L/G. Therefore, the compression energy is mainly effected by the stripper pressure. As stripper pressure increases from 1 to 2 bar, the compression energy for the liquefaction process decreases from 39 to 31 MW, as shown in Figure 12.

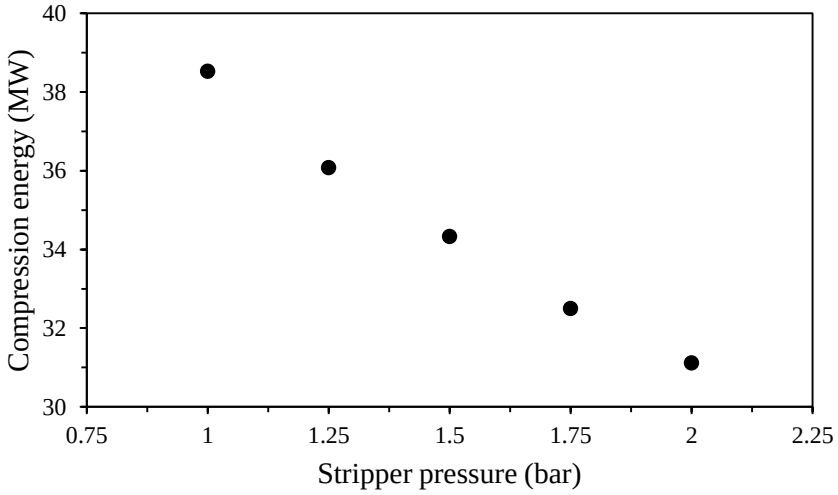

Figure 12. Effect of stripper pressure on compression energy

4.3. Power de-rate minimization

The power de-rate was derived from the simulation result for the integrated process using Aspen Plus combined with MATLAB to reduce cumbersome procedures. Figure 13 shows a 3-dimensional power de-rate graph for the backup turbine case obtained by manipulating the stripper operating pressure and L/G. Higher power de-rates are observed at lower operating pressure with lower L/G, whereas high operating pressures generally generate lower power de-rates regardless of L/G over a selected range. However, the minimum power de-rate using a backup turbine and steam extraction at the IP-LP crossover pipe occurs at a lower pressure with an intermediate L/G of 1.25 bar and 4.05 L/m^3, respectively. As the power de-rate in this integrated system was minimized by manipulating the most influential variables, it is predicated that the minimum achievable power de-rate that could be obtained by including all the possible variables would be similar. The details of the optimizations are listed in Table 9.

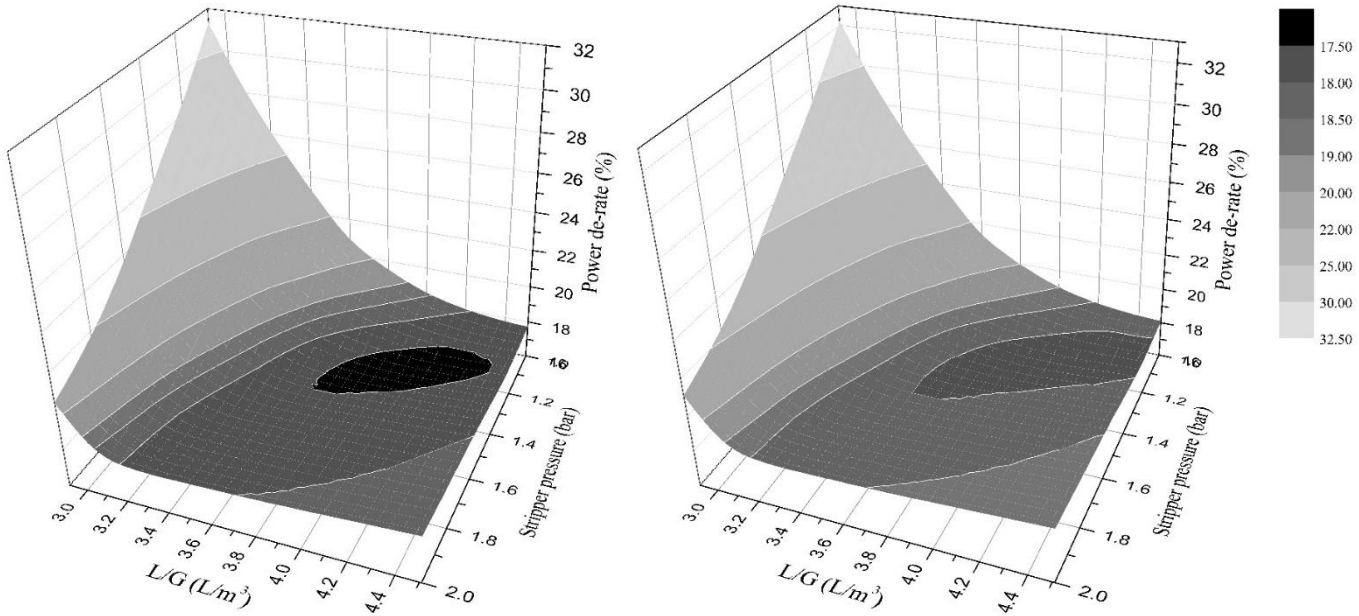

(a) (b)

Figure 13. Effect of stripper pressure and L/G on the power de-rate: (a) IP-LP crossover steam and (b) LP steam

Table 9. Optimization results

P_{str}	RB duty	Regen. E	RB T	Opt. L/G	$\dot{m}_{ex}$	$P_{bt,ratio}$	CE	Power output [1]	BT power	D [2]
bar	GJ/hr	GJ/tonCO_2	℃		ton/hr		kW	kW	kW	%
1	1,494	3.77	102.2	4.51	671.9	6.2	38,523	420,864	70,164	17.7
1.25	1,380	3.49	108.6	4.05	625.5	5.0	36,075	431,183	59,171	17.4
1.5	1,334	3.37	114.0	3.72	608.9	4.2	34,328	435,509	52,488	17.5
1.75	1,309	3.31	118.7	3.31	601.9	3.7	32,504	437,833	47,453	17.7
2	1,298	3.28	122.8	3.46	599.4	3.2	31,116	439,187	43,377	17.9

[1] Plant power output with CO_2 capture process

[2] Net plant power with CCS = Power output + Backup turbine power − Compression energy

Lowering the regeneration energy has been at the core of research on the capture process and many researchers improved the regeneration energy through process modifications and alternatives. Figure 14 shows the relationship between the power de-rate and regeneration energy of the capture process. In general, an integrated process with a lower regeneration energy tends to have a lower power de-rate; however, the minimum power de-rate does not occur at the condition that generates the lowest regeneration energy. The minimum power de-rate is 17.4%, which is 0.5% lower than that at the lowest regeneration energy with a stripper pressure of 2 bar and a L/G of 3.24 L/m^3. This result is significantly different from previous research that proposed higher stripper pressures for optimum operating conditions. This indicates that the optimum operating conditions for the unit processes (capture and liquefaction processes) are different from those for the integrated process owing to the steam extraction process.

In the stripper reboiler, the heat duty for solvent regeneration decreased with increasing stripper pressure, whereas its temperature increased. Higher temperatures in the reboiler require steam with a higher temperature and thus with a higher pressure. Therefore, the turbine train in the steam cycle is able to reduce the power output loss more than when the lower stripper pressure is used by extracting less steam, as shown in Figure 15. However, the expansion ratio of the backup turbine in the steam extraction unit is decreased. Furthermore, the compression energy in the liquefaction process decreased with increased

stripper pressure. This is why the optimum condition for the power de-rate occurred at a lower stripper pressure even though more extracted steam and compression energy are required. The operating conditions for the lowest steam extraction are not equivalent to those for the minimum power de-rate.

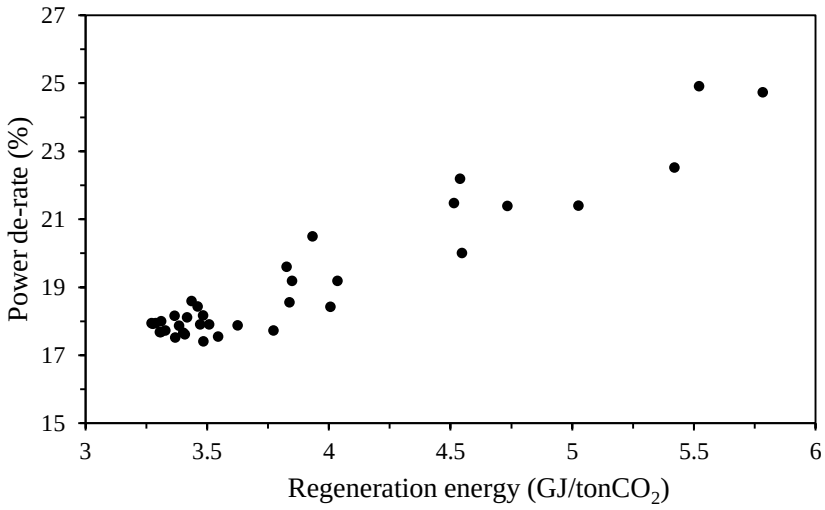

Figure 14. Power de-rate at different regeneration energies

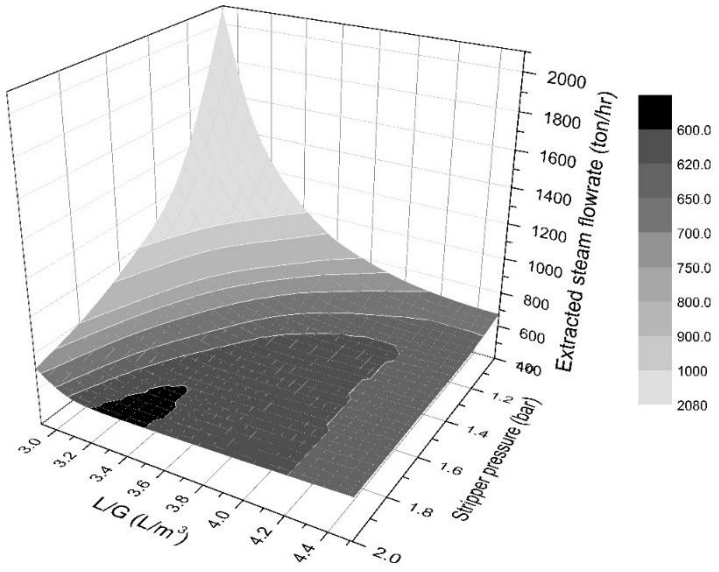

Figure 15. Effect of stripper pressure and L/G on extracted steam flowrate

CHAPTER 5. Conclusion

CCS is considered a realistic near-term technology to decelerate global warming. Unfortunately, the power de-rate caused by the reboiler heat duty and compression energy is an obstacle to CCS implementation. In this study, power de-rate minimization was performed by manipulating influential operating variables. A simulation of a 550 MWe supercritical coal-fired power plant with a post-combustion amine-based capture process and liquefaction process was carried out based on the data for a 0.1 MW CO_2 capture pilot plant. The stripper pressure and L/G ratio were chosen as the manipulating variables by variable evaluation. The results showed that the stripper operating pressure is the most influential operating variable that affects not only the capture process but also the liquefaction process. In addition, the regeneration energy is sensitive to L/G and an optimum minimum value was observed for each stripper pressure. As the stripper pressure increased, the regeneration energy in the capture process and the compression energy in the liquefaction process decreased. Extraction of a minimum amount of steam for reboiler from the steam cycle reduces power output loss in turbine train. However, an increased temperature in the reboiler requires higher quality steam, which decreases the expansion ratio of the backup turbine and thus recovers less power. Consequently, the total power de-rate is minimized when operating at a lower stripper pressure and an optimum L/G ratio of 1.25 bar and 4.05 L/m^3, respectively, with steam extracted from the

IP-LP crossover pipe and using option (b) for the steam extraction unit. The suggested operating conditions are different from the optimum conditions for the unit processes (capture and liquefaction processes), which are the highest pressure of 2 bar. Importantly, process control is essential to maintain a low power de-rate when operating at the lower stripper pressure because severe power de-rates may occur when operating at unsuitable L/G ratios. The minimum power de-rate was reduced to 17.4%.

Reference

(1) (a) Intergovernmental Panel on Climate Chagne, *Climate Change 2014*: *Mitigation of Climate Change*, 2014. (b) IEA, *How the energy sector can deliver on a climate agreement in Copenhagen*, 2009.

(2) International Energy Agency, Energy Technology Perspective 2012. *OECD/IEA* 2012.

(3) Elliott, T. C.; Chen, K.; Swanekamp, R. *Standard Handbook of Powerplant Engineering*; McGraw-Hill Education, 1998.

(4) Metz, B.; Davidson, O.; De Coninck, H.; Loos, M.; Meyer, L. IPCC, 2005: IPCC special report on carbon dioxide capture and storage; Prepared by Working Group III of the Intergovernmental Panel on Climate Change: Cambridge, United Kingdom and New York, NY, USA, 2005; 442 pp.

(5) Lucquiaud, M.; Chalmers, H.; Gibbins, J. Capture-ready supercritical coal-fired power plants and flexible post-combustion CO_2 capture. *Energy Procedia* **2009**, 1, 1411-1418.

(6) Lucquiaud, M.; Gibbins, J. Effective retrofitting of post-combustion CO_2 capture to coal-fired power plants and insensitivity of CO_2 abatement costs to base plant efficiency. *Int. J. Greenhouse Gas Control* **2011**, 5, 427-438.

(7) Harkin, T.; Hoadley, A.; Hooper, B. Reducing the energy penalty of CO_2 capture and compression using pinch analysis. *J. Cleaner Prod.* **2010**, 18, 857-866.

(8) Hanak, D. P.; Biliyok, C.; Yeung, H.; Białecki, R. Heat integration and exergy analysis for a supercritical high-ash coal-fired power plant integrated with a post-combustion carbon capture process. *Fuel* **2014**, 134, 126-139.

(9) Khalilpour, R.; Abbas, A., HEN optimization for efficient retrofitting of coal-fired power plants with post-combustion carbon capture. *Int. J. Greenhouse Gas Control* **2011**, 5, 189-199.

(10) Liew, P. Y.; Klemeša, J. J.; Doukelis, A.; Zhang, N.; Seferlis, P. Identification of process integration options for CO_2 capture in Greek lignite-fired power plant. *Chem. Eng. Trans.* **2014**, 39, 1447-1452.

(11) Sanpasertparnich, T.; Idem, R.; Bolea, I.; deMontigny, D.; Tontiwachwuthikul, P. Integration of post-combustion capture and storage into a pulverized coal-fired power plant. *Int. J. Greenhouse Gas Control* **2010**, 4, 499-510.

(12) Dave, N.; Do, T.; Palfreyman, D.; Feron, P. H. M. Impact of liquid absorption process development on the costs of post-combustion capture in Australian coal-fired power stations. *Chem. Eng. Res. Des.* **2011**, 89, 1625-1638.

(13) Liang, H.; Xu, Z.; Si, F. Economic analysis of amine based carbon dioxide capture system with bi-pressure stripper in supercritical coal-fired power plant. *Int. J. Greenhouse Gas Control* **2011**, 5, 702-709.

(14) Cifre, P. G.; Brechtel, K.; Hoch, S.; García, H.; Asprion, N.; Hasse, H.; Scheffknecht, G. Integration of a chemical process model in a power plant

modelling tool for the simulation of an amine based CO_2 scrubber. *Fuel* **2009**, 88, 2481-2488.

(15) Eslick, J. C.; Miller, D. C. A multi-objective analysis for the retrofit of a pulverized coal power plant with a CO_2 capture and compression process. *Comput. Chem. Eng.* **2011**, 35, 1488-1500.

(16) Van Peteghem, T.; Delarue, E. Opportunities for applying solvent storage to power plants with post-combustion carbon capture. *Int. J. Greenhouse Gas Control* **2014**, 21, 203-213.

(17) Patiño-Echeverri, D.; Hoppock, D. C. Reducing the energy penalty costs of postcombustion CCS systems with amine-storage. *Environ. Sci. Technol.* **2012**, 46, 1243-1252.

(18) Liebenthal, U.; Linnenberg, S.; Oexmann, J.; Kather, A. Derivation of correlations to evaluate the impact of retrofitted post-combustion CO_2 capture processes on steam power plant performance. *Int. J. Greenhouse Gas Control* **2011**, 5, 1232-1239.

(19) Zhang, K.; Liu, Z.; Wang, Y.; Li, Y.; Li, Q.; Zhang, J.; Liu, H. Flash evaporation and thermal vapor compression aided energy saving CO_2 capture systems in coal-fired power plant. *Energy* **2014**, 66, 556-568.

(20) House, K. Z.; Harvey, C. F.; Aziz, M. J.; Schrag, D. P. The energy penalty of post-combustion CO_2 capture & storage and its implications for retrofitting the U.S. installed base. *Energy Environ. Sci.* **2009**, 2, 193-205.

(21) Ciferno, J. Pulverized Coal Oxycombustion Power Plants. Final Report, revised August 2008.

(22) Haar, L.; Gallagher, J. S.; Kell, G. S. NBS/NRC steam tables: Thermodynamic and transport properties and computer programs for vapor and liquid states of water in SI units; *Hemisphere:* Washington, DC, 1984; 320 pp.

(23) Lim, Y. Process Design for CO_2 Capture from Coal-fired Plant and its Transport via Ship. Ph.D. dissertation, The Seoul National University, 2011.

(24) Hikita, H.; Asai, S.; Ishikawa, H.; Honda, M. The kinetics of reactions of carbon dioxide with monoethanolamine, diethanolamine and triethanolamine by a rapid mixing method. *Chem. Eng. J.* **1977**, 13, 7-12.

(25) Lee, U.; Yang, S.; Jeong, Y. S.; Lim, Y.; Lee, C. S.; Han, C. Carbon dioxide liquefaction process for ship transportation. *Ind. Eng. Chem. Res.* **2012**, 51, 15122-15131.

(26) Heggum, G.; Weydahl, T.; Roald, W.; Mølnvik, M.; Austegard, A. CO_2 conditioning and transportation. *Carbon Dioxide Capture for Storage in Deep Geologic Formations* **2005**, 2, 925-936.

(27) Alabdulkarem, A.; Hwang, Y.; Radermacher, R. Energy consumption reduction in CO_2 capturing and sequestration of an LNG plant through process integration and waste heat utilization. *Int. J. Greenhouse Gas Control* **2012**, 10, 215-228.

(28) Cousins, A.; Wardhaugh, L.; Feron, P. A survey of process flow sheet modifications for energy efficient CO_2 capture from flue gases using chemical absorption. *Int. J. Greenhouse Gas Control* **2011**, 5, 605-619.

(29) Rochelle, G. T. Thermal degradation of amines for CO_2 capture. *Curr. Opin. Chem. Eng.* **2012**, 1, 183-190.

(30) Davis, J. Thermal degradation of aqueous amines used for carbon dioxide capture. Ph.D. dissertation, The University of Texas at Austin, 2009.

Abstract in Korean (국문초록)

이산화탄소 포집 및 저장 기술 (CCS)은 온실가스 저감 및 기후 변화 대응을 위한 주요한 기술로써 전세계적인 관심을 받고 있다. 특히, 연소 후 이산화탄소 습식 포집 공정은 기존의 석탄 화력 발전소에 적용할 수 있는 기술로 다른 포집 기술에 비하여 경제적 이점을 가지고 있다. 더욱이 MEA (Monoethanolamine) 수용액을 이용한 포집 기술은 다른 공정들에 비해 잘 알려져 있으며 파일럿 플랜트 단계까지 실행된 바 있다. 하지만 흡수제 재생 및 이산화탄소 액화공정에 필요한 열과 에너지는 스팀 추출 및 발전 에너지 사용을 통해 화력발전소 출력의 30 %에 이르는 감소를 야기하며, 이를 power de-rate 라고 한다. Power de-rate는 발전소에의 CCS 도입을 막는 주요한 장애 요인으로 꼽힌다. 본 연구에서는 power de-rate 감소를 위해 공정 시뮬레이션을 기초로 한 발전–포집–액화 통합 공정의 파라미터 최적화 연구를 수행하였다. 550 MWe 발전소, 포집 및 액화 단위 공정 모델링을 Aspen plus V7.3을 통해 진행하였다. 특히 포집 공정은 KEPCO E&C의 0.1 MW 급 이산화탄소 포집 파일럿 플랜트의 모델링 및 운전 data를 바탕으로

설계하여 신뢰도를 높였다. 조작 가능 변수들의 power de-rate에 대한 평가를 통해 탈거탑 압력과 L/G 비를 조작 변수로 선정하였다. 스팀 추출을 위한 유닛은 감압을 위해 터빈 및 감압밸브를 이용한 두 가지 대안을 고려하였으며, 스팀 추출 위치는 IP-LP crossover pipe 및 첫 번째 LP 터빈을 선정하고 분석하였다. 연구 결과, 최적 운전 조건에서 power de-rate는 17.4%로 감소하였으며 이 때의 운전 조건은 1.25 bar의 탈거탑 운전 압력과 4.05 L/m^3의 L/G 비 이었다. 스팀 추출은 IP-LP crossover pipe에서 터빈을 이용하였을 때 최저 값을 보였다. 이는 기존의 연구 결과에서 단위 공정의 최적 운전 조건으로 제시하였던 2 bar의 고압이 아닌 1.25 bar의 중-저압을 통합 공정의 새로운 최적 운전 조건으로 제시하며 통합 공정에 대한 평가의 중요성을 보여 주었다.

주요어 : 발전량 감소, CCS 레트로핏, 연소 후 CO_2 포집, 운전 변수 평가, 다변수 최적화, 파라미터 최적화

학 번 : 2013-20980